

A 4×1 GHz Array Acousto-Optical Spectrometer for air- and spaceborne observations in the submm-region

J. Horn^{(2),(1)}, C. Macke⁽¹⁾, F. Schlöder⁽¹⁾, F. Schmüling⁽¹⁾, O. Siebertz⁽¹⁾
and R. Schieder⁽¹⁾

⁽¹⁾: I. Physikalisches Institut, Universität Köln,
Zülpicher Str. 77, 50937 Köln, Germany

⁽²⁾: University of California at Los Angeles,
405 Hilgard Av, CA 90024 Los Angeles, USA
email: horn@jupiter.astro.ucla.edu

March 17, 1998

Abstract

In this paper an array acousto-optical spectrometer (AOS) with four 1 GHz bands and a frequency channel spacing of 1 MHz is presented. The test results of the array AOS are comparable to those of the space-qualified AOS for the Submillimeter Wave Astronomy Satellite (SWAS). Allan variance tests, longtime integration tests and investigations of the relative stability between the four bands are presented. The Allan variance minimum time was found to be at least 1000s, which is one of the best results observed for broadband AOSs so far. Performance tests of the different bands revealed an identical frequency response. Therefore the relative stability of two simultaneous measured baselines is extraordinary, so that correlated noise can be eliminated efficiently. Recently the Array AOS has been in operation for 2 months at the IRAM 30m telescope. From this test-run, several results present the competitiveness of AOSs compared to filterbanks and hybrid autocorrelators. In an upgraded design concept the second generation array AOS will be more compact and reliable. This version will be operated not only on ground-based observatories like KOSMA or AST/RO, but also on airborne and spaceborne facilities like SOFIA and FIRST.

Keywords: Radio Astronomy, Acousto-Optical Spectrometer, Backends, Radiometers, Heterodyne Instrumentation, Array Receivers

1 Introduction

In the recent years the worldwide development of large bandwidth, multi-frequency or multi-beam receivers has incited a demand on corresponding backends. In the submillimeter wavelength range and of course in the THz region, the requirements in bandwidth increase drastically. At the same time it might be necessary to have relatively high resolution at the same time, for frequency surveys e. g. Such requirements hold for atmospheric observations as well, because most atmospheric lines tend to have extended line wings together with rather narrow peaks at the center of the lines. Future airborne or spaceborne observatory projects like SOFIA¹ or FIRST² depend crucially on versatile backend developments in order to achieve a most economic usage of the available equipment with optimum scientific return. At KOSMA³ a new superconducting mixer array frontend with 2×4 channels at 490 and 810 GHz is under development, so that the number of backends needed grows accordingly.

In this paper, the recent development of an array acousto-optical spectrometer (AOS) with 4×1 GHz bandwidth is presented. Its optical layout is discussed with respect to the required specifications for normal operation at radio observatories. The laboratory test results have proven that the specifications have been achieved. To check the performance of the array AOS during observations at a telescope, it has been installed at the IRAM 30m telescope for a two-month test period this early summer. The outcome of these tests did also show an excellent agreement with the expected performance.

¹Stratospheric Observatory for Infrared Astronomy

²Far InfraRed Space Telescope

³Kölnener Observatorium für SubMm Astronomie

2 System Design

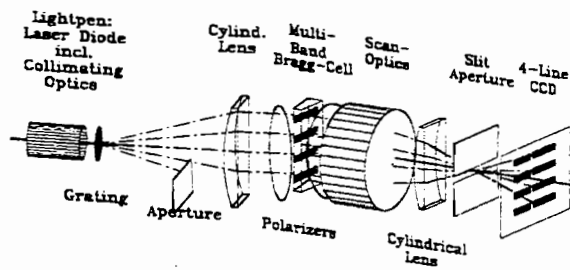


Figure 1: *The principal optical design of the KOSMA 4×1 GHz array AOS*

The principal design of the array AOS is similar to those of the standard KOSMA single-band AOSs such as the one for the Submillimeter Wavelength Astronomy Satellite (SWAS), (Klumb et al., 1994). As shown in Fig. 1, four intermediate frequency (IF) signals, are fed to the array Bragg cell which is made out of a single LiNbO₃ crystal. Through the piezoelectric transducer, an acoustic wave inside the crystal is induced. The acoustic wave produces a periodically

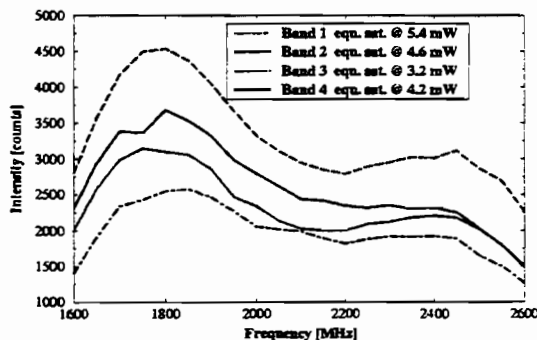


Figure 2: *The bandpasses of the four bands of the array AOS measured with a synthesizer*

varying diffraction index inside the crystal. At the associated phase grating, monochromatic laser light, four beams for each acoustic

active zone produced by means of a holographic grating, is diffracted under the Bragg condition. The first order diffracted laser light is then imaged onto the CCD by means of a scan optics and a cylindrical lens. The Bragg cell is operated in shear wave mode, enabling efficient light scatter reduction by means of two crossed polarizers. The deflected light beams are then imaged onto four independent and parallel CCD lines. Especially the second cylindrical lens is responsible for the exact matching of the beams onto the corresponding CCD line.

With this setup, a high efficiency has been achieved, as can be seen in Fig. 2. The IF power, which is necessary to bring all pixels equalized in saturation, is well below 6 mW for all four bands, yielding a maximum total power level on the crystal of less than 20 mW, which is comparable to the amount of one of our single-band AOSs. Furthermore, the bandpasses have a 3 dB shape over the 1 GHz band, which could be further smoothed by means of an r. f. equalizer if necessary. The problem in such an efficient optical layout is the increasing amount of light scatter collected on the CCD. Former studies have shown, that a strong light scatter level decreases the spectroscopic stability of a spectrometer, which is measured by the maximum total power integration time as a result of the so-called Allan-variance plot (Schieder et al., 1989). By introducing a slit aperture at the beam crossing point, the scattered light could be nearly eliminated in all four bands simultaneously. As a result, extraordinary spectroscopic stabilities have been achieved with the array AOS, as is described in the next section.

To avoid any overlap of the acoustic beams, which would cause unwanted crosstalk between the bands, the transducers are spaced by 1.6 mm. The residual crosstalk measured

is below -30 dB between the bands and purely of electrical origin. This has been confirmed with measurements done by the supplier of the cell, measuring the electrical crosstalk of the IF matching circuit (GEC Marconi, 1995).

3 Performance Tests

3.1 Laboratory tests

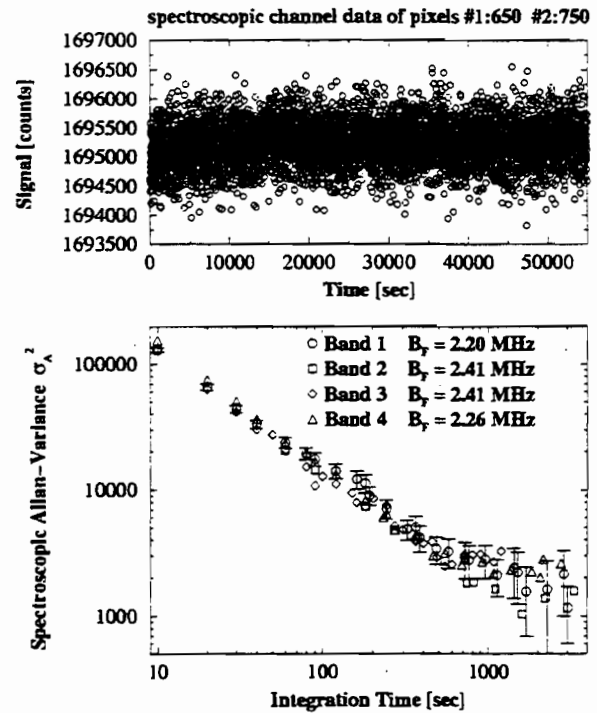


Figure 3: Data of one spectroscopic channel and the spectroscopic Allan-variance plot

One important test parameter is the minimum time of the Allan-variance plot, or the maximum total power integration time, which has been found to be up to 1000 s using a noise source under thermally stable conditions, see Fig. 3. Compared with normal operation, where a minimum time of above 100 s

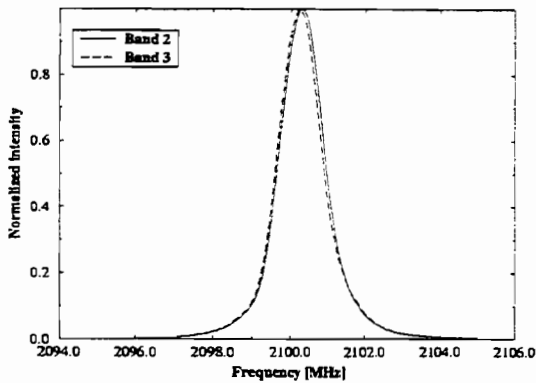


Figure 4: The filtercurves of two vertically adjacent pixels (in two adjacent AOS bands)

is enough to guarantee proper measurements, the array AOS is therefore not limiting the measurements.

The identical performance of the different bands has been tested in various ways. First, the bandpasses have shown, that the IF power response of the bands is equal within 2 dB. The differences are partly due to the grating and partly to alignment tolerances. The frequency response has been tested to be identical for two bands as well. Therefore, filtercurves of the same pixel in two adjacent bands have been measured, see Fig. 4. The strong overlap of these curves indicates high radiometric correlation, which can be calculated to be 99.8 %, (Horn, 1997).

To make sure, the filtercurves show such strong overlap along the whole frequency band, the frequency nonlinearity, which typically exist in AOSs, has to be taken into account. This nonlinearity has been measured in all four bands to be identical over the whole 1 GHz bandwidth. Furthermore, although it is very low about 1 frequency channel along the full bandwidth it can be further reduced to about 0.1 channels by means of a prism. This identical frequency response of the

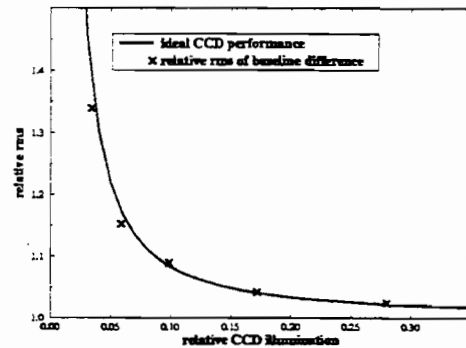
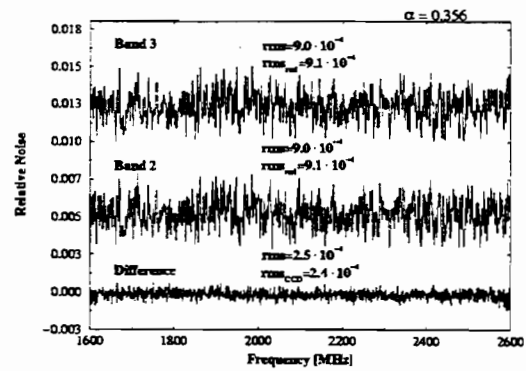


Figure 5: The top graph shows simultaneously measured noise spectra in both AOS bands at high illumination level together with the difference spectrum. The noise of such difference spectra, measured at various illumination levels, has been scaled down to the contribution of one single CCD relative to radiometric noise, as shown in the lower graph

various bands is a precondition, to eliminate identical noise apparent in two different bands. To check this performance, the output of a noise source has been split up and fed into two bands of the array AOS. Subtracting both simultaneously measured noise spectra, only the detector resides. The theoretical noise of the CCD has been calculated to be identical to the noise of the difference spectrum. The difference spectrum in Fig. 5 directly reflects the identical frequency response of the 1 GHz bands.

Decreasing the illumination level, that is, the IF drive power level at the Bragg cell the detector noise of the AOS, which consists mainly of shot- and dark-noise of the CCD, should increase. In that sense, one can define a noise dynamic range as the illumination level, where the CCD adds less than 1 dB noise to the radiometric noise.

The noise spectra described above have been repeated at various IF drive power levels of the noise source. The lower plot in Fig. 5 shows the noise contribution of the CCD relative to radiometric noise. One can see, that the noise is increased by 1 dB at an illumination level of about 5-6 %, yielding a noise dynamic range of at least 12 dB. If the CCD is illuminated below this level, the noise increases drastically, as is indicated by the steep slope of the curve.

3.2 Astronomical measurements

```

1907: 1 IRC+10216 13CO(2-1) IRAM-30M-B31 O: 15-MAY-1997 R: 15-MAY-1997
RA: 9:45:14.800 DEC: 13:30:40.00 (1950.0) Offs: 0.0 0.0 Eq
Unknown Tau: 0.2870 Tsys: 462.0 Time: 15.00 El: 32.54
N: 512 FO: 256.5 VO: -27.00 Dv: 1.360 LSR
FO: 220398.682 DI: -1.000 FI: 228262.941

```

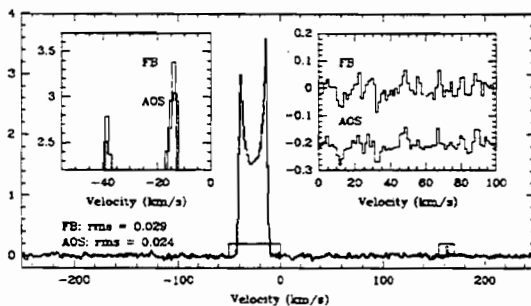


Figure 6: A measurement of $^{13}\text{CO}(1-0)$ in IRC+10216 to test the calibration scale of the AOS compared to the filterbank

The calibration of the array AOS has also been checked, using well known sources, like IRC+10216, where the line peak tempera-

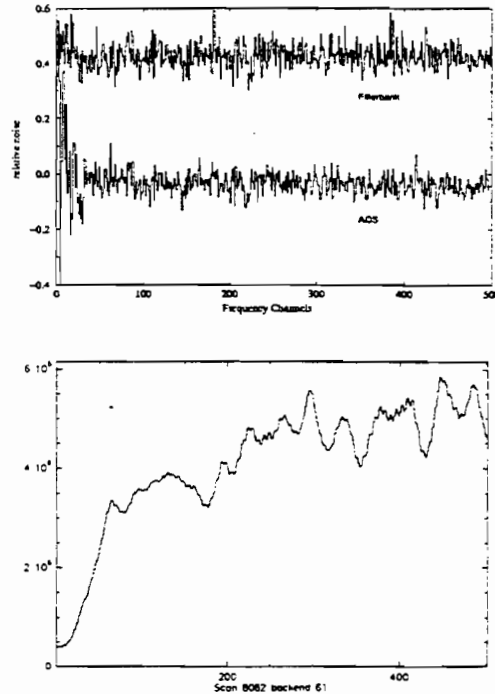


Figure 7: The baseline quality at illumination levels below the specified range for the AOS; the lower spectrum is measured with the AOS, the upper one with the filterbank. The bandpass shows a 500 MHz band measured with the AOS, on Hot Load. Saturation is reached at about $25 \cdot 10^6$ counts, the 12 dB noise dynamic range limit is therefore reached at roughly $2 \cdot 10^6$ counts.

ture is known. The IRAM filterbanks have been used in parallel to directly compare the results. For an interpretation, one has to take into account, that the AOS has a lower resolution (resolution bandwidth 1.5 MHz) than the filterbank (resolution bandwidth 1.0 MHz). In AOS spectra, narrow line features must therefore be frequency diluted and show a lower peak response as lines measured with the filterbank. This is nicely visible in Fig.6, where the curve with the lower peak response has been measured with the array AOS. The identical response in the flat part

of the line center demonstrates on the other hand that the calibrations are identical, as can be seen in the left zoom. The velocity range from 0 to 100 km s⁻¹ zoomed, shows that features in the baselines are also nearly identical. The ratio of the RMS values is consistent with the ratio of the fluctuation bandwidths, which is 2.3 MHz for the array AOS and 1.4 MHz for the filterbank (Wild, 1995). For the calculation of the RMS values, line window have been set as are indicated in Fig. 6, so that the bad filterbank channel is not regarded.

During normal observations after installation of the array AOS, B. Lazareff et al. have generated some radiometric test data at 500 MHz bandwidth on Venus, again using the filterbanks in parallel, see Fig. 3.2. One can see excess noise at the left edge of the array AOS spectrum, whereas the Filterbank has only little of this excess noise.. The reason, that this only becomes visible at the edges of the spectra is due to the low IF power at the edges of the spectrum, which is fed into the AOS as is shown in Fig. 3.2. The bandpass for the 500 MHz band is shown in the lower graph. The 12 dB noise dynamic range limit is reached at about 2 10⁶ counts. This limit has been calculated, assuming 3 dB difference between Hot Load and sky and about 25 10⁶ counts for saturation. The excess noise indicates the limits of the CCD, which has to be illuminated above the 12 dB noise dynamic range limit, in the way it is operated at the moment. One could think of improvements in the CCD itself, in terms of looking for a device with better noise characteristics. But then the 12 Bit Analog to Digital Converter (ADC) used is the limiting factor, as the inherent differential non-linearity (DNL) then contributes to the noise. The effect of the DNL is already obvious at the very left edge, below 1 10⁶

counts of the bandpass, or within the first 20 frequency channels, due to the power difference between On- and Off-position on Venus, (Jarnot R.F., 1988). The effect of DNL can easily be reduced by inserting 14 or 16 Bit ADCs instead of the 12 Bit ADC used in this prototype version. A detailed discussion of the impact of the DNL on the noise performance at low illumination levels will be published soon. Furthermore, the DNL affects the baseline only when there are power offsets between the On and the Off position. Depending on how strong these offsets are, the DNL might already become a significant contributor to excess baseline noise next to the CCD. Sensitive measurements therefore require higher Bit resolution ADCs. When using 14 or 16 Bit ADCs, it would also make sense to improve the CCD characteristics or the readout speed, so that a noise dynamic range of 15 dB or more could be achieved. Furthermore one

```

2838 1 SGRCAOS 13CO(1-0) IRAM-30M-B51 0: 17-MAY-1997 R: 17-MAY-1997
RA: 17:41:23.661 DEC: -29:14:22.00 (1950.0) Ori: -0.250 0.0 Eq
Unknowns: Tau: 7.5160E-02 Tsys: 302.2 Time: 10.00 El: 23.79
N: 501 IC: 251.0 VO: 0.0000E+00 Dv: -2.829 LSR
FO: 11C201.37C DF: 1.040 FI: 113197.118

```

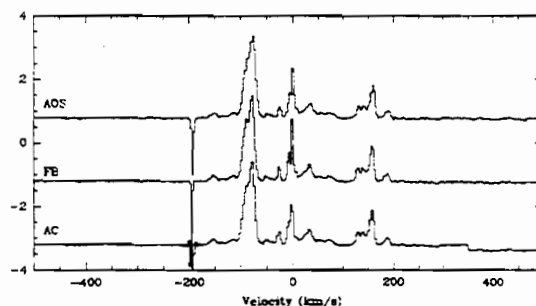


Figure 8: *Simultaneous measurements at 500 MHz bandwidth with the array AOS, filterbank, and hybrid autocorrelator*

can think of introducing an r. f. equalizer to reduce the bandpass variation of the AOS from 3 dB at the moment to about 1 dB. Filterbank spectra would also be affected

by DNL if the digitization is done with ADCs. At the IRAM filterbanks however, Voltage Controlled Oscillators with following Counters are in use. The excess noise at the edges is therefore only detector noise.

Further measurements on Sgr C using 500 MHz bandwidth have been performed with the array AOS, filterbank, and hybrid autocorrelator in parallel, see Fig. 8. As in Fig. 6, one can see the frequency dilution of the array AOS due to its lower resolution compared with the filterbank. This becomes visible in the absorption feature at 0 km s^{-1} as well as at the IF spike at -200 km s^{-1} . Besides platforming, the autocorrela-

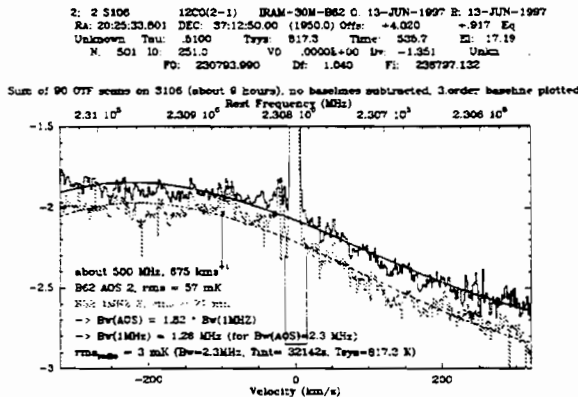


Figure 9: *Simultaneous On-the-fly (OTF) measurements at 500 MHz bandwidth with the array AOS (top) and the filterbank (bottom)*

tor shows much lower resolution as the nominally expected 1.25 MHz. One can see this at the absorption feature, which does not become visible in this spectrum, as well as at the absorption spike. This is probably caused by the process of smoothing the data with some apodization to suppress the sidelobes, which become visible if narrow lines are observed.

Schneider et al. mapped S106 on-the-fly (OTF). Summing up all 90 OTF scans, yields

to the spectrum shown in Fig. 9. After a total integration time of about 9 hours, the filterbank spectrum shows several bad channels. The AOS spectrum shows some excess noise at the right edge, where the illumination level is below the specified 12 dB, otherwise, the baselines would be exactly identical at this edge as they are for the rest of the baseline.

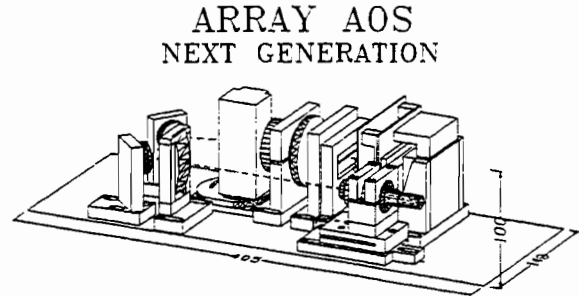


Figure 10: *The mechanical concept of the next generation array AOS. The optical parameters are the same as with the first version.*

The array AOS presented herein served as a prototype and showed already very good results. Nevertheless, the next versions e.g. for AST/RO or KOSMA, are being redesigned to make them more compact and to have already a kind of 'engineering model' for missions like FIRST or SOFIA. The principal optical setup of the next generation AOS is shown in Fig. 10. It differs from the first version only in the folded optical layout and some means to facilitate the alignment.

4 Conclusions

The performance tests have shown, that the concept of the KOSMA array AOS is suitable for radio astronomical applications at millimeter and submillimeter observatories. Even for heterodyne receiver arrays in the

THz region, which can be implemented at SOFIA, the array AOS provides sufficient frequency coverage to allow the detection of extragalactic signals. At 2 THz, the bandwidth of 1 GHz corresponds to 150 km s^{-1} , which is still sufficient for most galactic observations. If the velocity range needs to be larger, the AOS bands could also be joint together as done with hybrid autocorrelators. The identical noise performance of the different bands, if illuminated properly, are a decisive precondition to avoid different noise levels in the hybrid band. As there are no obvious different drifts within the two bands, platforming should not arise. At the moment, an IF processor is under development, to split a 2 GHz IF band and to feed the signals into two AOS bands. The performance of hybrid spectra can then directly be tested.

To improve the noise dynamic range of the AOS from now 12 dB to at least 15 dB are on the way, enhancing the Bit resolution of the analog to digital converter and the readout speed of the CCD.

5 Acknowledgements

We like to thank IRAM and the 30m staff to realizing the test-run with the array AOS, especially B. Lazareff and G. Paubert as well as N. Schneider, C. Kramer et al. and H. Wiesemeyer for providing additional test data. The array AOS has partly been financed through grant SFB 301 of the DFG (Deutsche Forschungsgemeinschaft).

6 References

GEC-Marconi, *Test Results of the array Bragg Cell*, Device Identity: Y-36-7436-02, Serial No.: MRQ IS001 (1995)

Horn J., *The development of an array acousto-optical spectrometer*, Ph.D. thesis, Univ. Köln (1997)

Jarnot R.F., Technical Note 1, JPL Microwave Atmospheric Sciences Group (Aug. 18., 1988)

Klumb M., Frerick J., Tolls V., Schieder R., Winnewisser G., *The SWAS Acousto-Optical Spectrometer*, SPIE Vol. 2268, p305 (1994)

Schieder R., Tolls V., Winnewisser G., *The Cologne Acousto-Optical Spectrometers*, Exp. Astron. 1: 101-121 (1989)

Schneider N., Kramer C. et al., *IRAM project 39/97* (1997)

Wild W., *The 30m Manual*, Version 1.0, IRAM Granada (1995)